Available online at www.sciencedirect.com

SCIENCE DIRECT

Biochimica et Biophysica Acta 1758 (2006) 653–665

BIOCHIMICA ET BIOPHYSICA ACTA BBA

http://www.elsevier.com/locate/bba

Desolvation map of the i-face of phospholipase A2

Yu-Cheng Tsai, Bao-Zhu Yu, Yu-Zhen Wang, Junghuei Chen, Mahendra K. Jain *

Department of Chemistry and Biochemistry, University of Delaware, Newark, Delaware 19716, USA

Received 29 November 2005; received in revised form 6 March 2006; accepted 6 April 2006
Available online 20 April 2006

Abstract

The changes in the microenvironment of the Trp-3 on the i-face of pig pancreatic IB phospholipase A_2 (PLA2) provide a measure of the tight contact (Ramirez and Jain, Protein Sci. 9, 229–239, 1991) with the substrate interface during the processive interfacial turnover. Spectral changes from the single Trp-substituent at position 1, 2, 6, 10, 19, 20, 31, 53, 56 or 87 on the surface of W3F PLA2 are used to probe the Trp-environment. Based on our current understanding only the residue 87 is away from i-face, therefore all other mutants are well suited to report modest differences along the i-face. All Trp-mutants bind tightly to anionic vesicles. Only those with Trp at 1, 2 or 3 near the rim of the active site on the i-face cause significant perturbation of the catalytic functions. Most other Trp-mutants showed < 3-fold change in the interfacial processive turnover rate and the competitive inhibition by MJ33. Binding of calcium to the enzyme in the aqueous phase had modest effect on the Trp-emission intensity. However, on the binding of the enzyme to the interface the fluorescence change is large, and the rate of oxidation of the Trp-substituent with N-bromosuccinimide depends on the location of the Trp-substituent. These results show that the solvation environment of the Trp-substituents on the i-face is shielded in the enzyme bound to the interface. Additional changes are noticeable if the active site of the bound enzyme is also occupied, however, the catalytically inert zymogen of PLA2 (proPLA2) does not show such changes. Significance of these results in relation to the changes in the solvent accessibility and desolvation of the i-face of PLA2 at the interface is discussed.

Keywords: Interfacial kinetics; Processive turnover; I-face; Lipid-protein interaction; Phospholipase A_2

1. Introduction

The i-face[1] of interfacial enzymes is structurally and functionally different than their active site that carries out the steps of the catalytic turnover cycle [1,2]. Contact of the i-face to the interface facilitates the substrate accessibility, determines the interface preference and processivity, and mediates the allosteric effects of the interface on the steps of the interfacial turnover cycle. For example, tight contact of i-face of pig pancreatic phospholipase A2 (PLA2)[a] with the interface of anionic phospholipid bilayer permits the highly processive interfacial turnover [3–6] such that the interfacial turnover rate is > 10,000 higher than that in the aqueous phase [7].

As shown in Scheme 1, during the pre-steady state E to E* step the i-face of PLA2 binds tightly to the interface, and the steady state turnover occurs with the enzyme confined to the interface [1,2,5,6]. Such reaction progress in the highly processive scooting mode can be ensemble-averaged and analyzed to obtain the primary rate and equilibrium parameters for the interfacial turnover cycle events. Analyses show that the i-face of pig pancreatic phospholipase A_2 (PLA2) remains in contact with the substrate interface [8,9] to access the substrate [2]. Contact of the i-face modulates not only the interface preference [10], but also allosterically controls the turnover parameters of the catalytic cycle [11]. Higher affinity of E* for the substrate, compared to that for the E form in the aqueous phase, is the basis for the K_S^*-activation [12]. Also, the charge compensation of the cationic residues 53, 56 and 120 on the enzyme by the anionic charge at the interface induces the k_{cat}^*-activation [13]. These analyses are not possible if the enzyme is not tightly bound because the E to E* exchange induces the

Abbreviations: DC_7PC, 1,2-Diheptanoyl-*sn*-3-glycerophocholine; DMPM, 1,2-dimyristoyl-*sn*-3-glycerophosphomethanol; DTPM, 1,2-ditetradecyl-*rac*-3-glycerophosphomethanol; $DTSO_4$, 1,2-ditetradecyl-*rac*-3-glycero-sulfate; i-face, the interface binding surface of PLA2; MJ33, 1-hexadecyl-3-trifluoroethyl-*rac*-glycero-2-phosphomethanol; NBS, N-bromosuccinimide; octyl-Trp, octylester of tryptophan; PLA2, IB phospholipase A2 from pig pancreas; RET, fluorescence resonance energy transferred

* Corresponding author. Tel.: +1 302 831 2968; fax: +1 302 831 6335.
E-mail address: mkjain@udel.edu (M.K. Jain).

0005-2736/$ - see front matter © 2006 Elsevier B.V. All rights reserved.
doi:10.1016/j.bbamem.2006.04.003

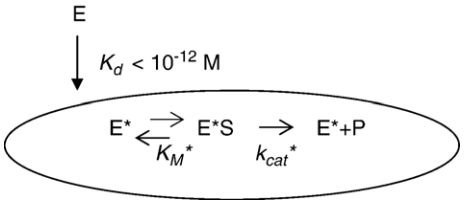

Scheme 1. Kinetic Scheme for the interfacial catalytic turnover by E* that remains confined to the interface during the processive steady state turnover in the scooting mode. With K_d <10^{-12} M [k_{off}/k_{on}] for the E to E* step the inter-vesicle exchange rate is negligible. The exchange rate of S* is also low if the CMC is low (<10^{-12} M for DMPM). Also both the extent and the rate of exchange of P* would be effectively negligible in the absence of an amphiphile that can counter-exchange. E*L mentioned in the text refers to the dead-end complex of E* with a substrate analog L such as MJ33, DTPM, or $DTSO_4$.

stationary phase reaction progress where the turnover path cannot be unequivocally assigned [5,14].

Structural and thermodynamic constraints of interactions along the i-face make it difficult, if not impossible, to adopt the methods that have been successful for the characterization of the functional states of enzymes in aqueous solutions. Although the solution NMR and crystallographic structures of PLA2 are in reasonable accord with each other [1,6,15–19], such results do not necessarily relate to the catalytically activated form of the enzyme at the anionic interface [5,6,20,21]. Current structural description of the interactions of the i-face of E* is based on indirect methods [1,2,22,23]. Unlike the active site of an enzyme, the i-face of PLA2 is believed to be a complex motif (Fig. 1). Its large relatively flat area of 1600 $Å^2$ makes short-range (< 5Å) high affinity contact with the interface of a bilayer or micelle. Such interactions must be accompanied by the substitution of solvated water at the i-face and the substrate interface by specific short range contacts with the ligands from the protein and the interface [24,25]. Exclusion of the solvent water from the contact region [8] could provide a basis for a water-free access route for the substrate in the interface to the active site of E*, and also for the mechanistically critical changes in the catalytic site [20,21] and for the allosteric coupling between the active site and the i-face functions [11–13].

In this paper we characterize spectral changes associated with interactions of i-face of several Trp-mutants with single Trp-substitutions on the surface of W3F PLA2 at 1, 2, 3, 6, 10, 19, 20, 31, 53, 56 or 87 (Fig. 1). Based on our current understanding only residue 87 is away from the i-face. Trp-substituent at all other positions are on, at or near the i-face, and therefore well suited to report modest differences along the i-face. Results show that the Trp-microenvironment depends on the position of Trp, which changes on the binding of the enzyme to DTPM vesicles to form E*, and further with the occupancy of the active site of E*L. The polarity and solvent accessibility of Trp in the bound enzyme increases as the probe moves away from the center of the i-face where the substrate-binding slot is localized. A surprising result is that the microenvironment of Trp in certain positions on the i-face also changes noticeably with the occupancy of the active site of the enzyme bound to the interface.

2. Materials and methods

2.1. Reagents

DC_7PC was from Avanti and NBS from Sigma. DMPM, DTPM and $DTSO_4$ were synthesized as described [3,26,27]. All other reagents were analytical grade. Concentrations of single Trp-mutants are based on $OD^{1\%}$ of 13 at 280 nm. Kinetic and spectroscopic protocols established before are outlined below and specific conditions for measurements are given in the text and figure legends. All measurements were carried out at pH 8.0 and 24 °C. Protocols for this study based on those established before [28,29], and only key differences are outlined below.

2.2. Construction and purification of the Trp-mutants of PLA2

Bert Verheij and Marcel Jenssen (Reijksuniversiteit, Utrecht) provided mutants #5 to #9 and #16 (Table 1). Their mutagenesis protocol in the *E. coli* expression system [30] was adopted with minor modifications for obtaining the other mutants (Table 1) in 3–10 mg/l. Valentin and Lambeau provided the pET-25b(+) plasmid template containing the pig pancreatic IB pro-PLA2 gene. Instructions of Quick Change II Site-directed Mutagenesis kit (Stratagene, La Jolla) were used to create plasmids carrying the following mutations: Mutation in WT was introduced for R6M, K10M and R6M/K10M. Similarly, the second mutation in W3F for Trp at 1, 2, 6, 10, 19, 20, 53, 56, 63 and 87 (Table 1) was introduced on the DNA template for the W3F PLA2 gene. The oligonucleotide primers (the bold-underlined codon indicates the location of mutation) used for

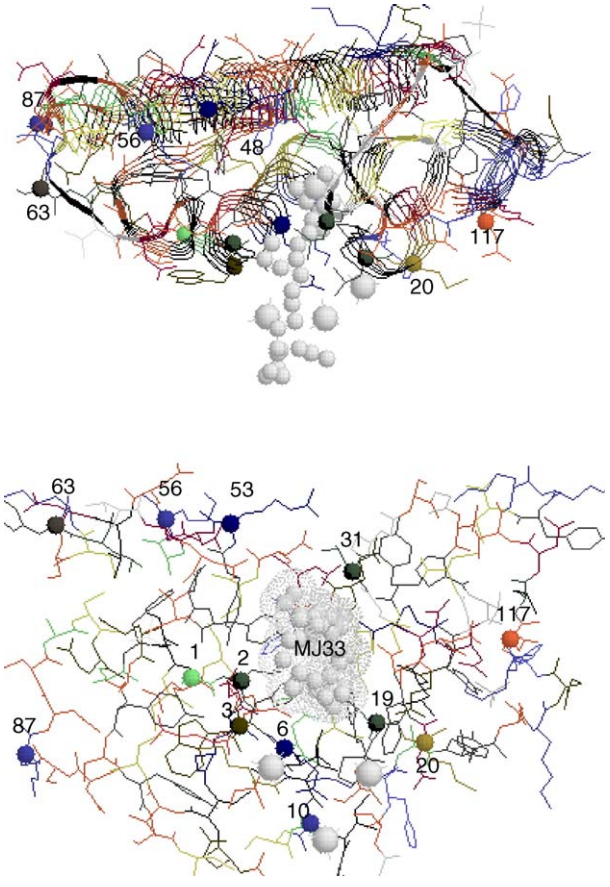

Fig. 1. Two orthogonal views of pig pancreatic 1B PLA2 from the anion-assisted homodimer (PDB 1FXF) with (gray circle) calcium, MJ33 and three phosphate-ions with (colored circles) Cα-atoms of the residues 1, 2, 3, 6, 10, 19, 20, 31, 53, 56, 63, 87 and 117. H48 (in top) is the catalytic residue. In the top view, the i-face is in the horizontal plane perpendicular to the plane of the paper. In the bottom view, the i-face is in the plane of the paper facing the reader.

Table 1
Catalytic parameters [a] for the Trp-substitution mutants of PLA2

#	Pig PLA2	v_o (s^{-1}) DMPM	$X_I(50)$* MJ33 DMPM	v_o (s^{-1}) DC7PC in	$X_I(50)$* MJ33 4 M NaCl
1	WT	300	0.0061	600	0.012
2	−R6M/K10M	30	0.043	180	0.025
3	−R6M	46	0.017	237	0.025
4	−K10M	64	0.02	237	0.006
5	−L31W	105	0.022	60	0.008
6	−N117W	237	.004	200	0.007
7	−N117W,D119Y	137	.005	155	0.005
8	−N117W,K116Y, D119Y	141	.006	154	0.005
9	W3F	160	0.011	105	0.013
10	−A1W	20	0.021	30	0.03
11	−L2W	6	0.009	74	0.018
12	−R6W	44	0.017	375	0.013
13	−K10W	48	0.019	104	0.016
14	−L19W	40	0.016	74	0.02
15	−M20W	65	0.011	114	0.012
16	−L31W	140	0.0005	21	0.02
17	−R53W	25	0.016	100	0.006
18	−K56M	41	0.013	200	0.011
19	−F63W	54	0.029	400	0.005
20	−K87W	48	0.023	160	0.005

[a] Uncertainty in the absolute values of these parameters is 30%, and 10% in individual measurements. Steady state rate v_o with DMPM is at 0.4 mM, and at 3 mM for DC_7PC.

the PCR reaction (16 cycles with Pfu Ultra HF DNA polymerase) to construct the mutant plasmids were:

5′-CCGCGGGCATTATGGCAGTTT**ATG**AGCATGATTAAGTGCG-CAATC-3′ **(R6M)**,
5′-GTTTCGTAGCATGATT**ATG**TGCGCAATCCCCCGGCAG-3′ **(K10M)**,
5′-GCATCAGTCCGCGGGCATTA**TTC**CAGTTTCGTAGCATGAT-TAAG-3′ **(W3F)**,
5′-GGCATCAGTCCGCGG**TGG**TTATTCCAGTTTCGTAGCATG-3′ **(A1W)**,
5′-GGCATCAGTCCGCGGGCA**TGG**TTCCAGTTTCGTAGC-3′ **(L2W)**,
5′-CCGCGGGCATTATTCCAGTTT**TGG**AGCATGATTAAGTGCG-CAATC-3′ **(R6W)**,
5′-TTCCAGTTTCGTAGCATGATT**TGG**TGCGCAATCCCCGGCAGT-CAC-3′ **(K10W)**,
5′-CCCGGCAGTCACCCC**TGG**ATGGATTTCAACAAC-3′ **(L19W)**,
5′-CCGGCAGTCACCCCTTG**TGG**GATTTCAACAACTATG-3′ **(M20W)**,
5′-CAGGACAACTGCTAC**TGG**GATGCCAAGAACCTGGAC-3′ **(R53W)**,
5′-AACTGCTACAGAGATGCC**TGG**AACCTGGACAGCTGTAAA-3′ **(K56W)**,
5′-CTGGACAGCTGTAAA**TGG**CTCGTGGACAATCCCTAC-3′ **(F63W)**,
5′-GAGATCACCTGCAACAGC**TGG**AACAATGCTTGTGAGGCC-3′ **(K87W)**.

The PCR products were transformed into XL-1 Blue competent cell and selected by incubating in LB-ampicillin agar medium. For each construct, correct mutation in the gene of the isolated plasmid was confirmed by DNA sequencing. The 0.45-kb mutant PLA2 gene was released by treating mPLA2-pET plasmid with restriction enzymes (*Hin*dIII and *Bam*HI from New England Biolab) that cleave at 57 bp upstream from the start codon and 4 bp down stream from the stop codon of inserted mutant PLA2 gene. The released mutant gene was then recloned into pAB3 expression vector with Quick ligase (New England Biolab). The target gene is composed of three continuous sections: GST promoter, GST gene and pro-mPLA2 gene. The advantage of fusing the GST promoter and GST gene with the pro-PLA2 gene is that the yield of the animal proPLA2 as a GST fusion protein in the bacterial expression system is improved to 10 to 30 mg/l.

After the reconstruction of the expression plasmid (mPLA2-PAB3), the plasmid was transformed into *E. coli* strain BL21 (Stratagene) for the mutant PLA2 expression. Single colony of the bacteria on LB-ampicillin agar plate (50 μg/ml) was picked and grown at 37 °C with 250 rpm shaking in 4L LB broth medium containing 50 μg/ml ampicillin. When the OD_{600} of the medium reached 0.6–0.8, 1 μM IPTG was added to induce protein expression and incubation continued for 6 more hours at 37 °C. Cells were then harvested by centrifugation at 6500 rpm in SLA-3000 for 15 min at 4 °C.

For cell lysis and subsequent isolation of inclusion bodies of the mutant protein, the cell pellet was resuspended in 200 ml buffer (50 mM Tris–HCl, pH 8.0, 50 mM NaCl, 1 mM EDTA, 0.5 mM freshly added PMSF) containing 1% Triton X-100 (v/v) and 1% sodium deoxycholate (w/v). The mixture was stirred at 4 °C for 20 min, and then sonicated for 15 cycles of 15 s on and 15 s off. The pellet was then collected by centrifugation at 9,000 rpm in 4 °C with GSA rotor for 10 min, and resuspended in 200 ml buffer containing 1% Triton X-100 (v/v) and 1% sodium deoxycholate (w/v) with stirring at 4 °C for 20 min. Collected pellet was resuspended in 200 ml buffer with 1% Triton X-100 (v/v), stirred at room temperature for 20 min, and then centrifuged under the conditions above. The pellet was then resuspended in 200 ml buffer without detergent and stirred at room temperature for 20 min. After centrifugation at 4 °C (supernatant discarded) the pellet of inclusion bodies was dissolved in 100 ml sulfonation buffer (6 M Guanidine–HCl, 0.3 M Na_2SO_3, 50 mM Tris–HCl, pH 8.0), and then 5 ml of 50 mM Ellman's reagent was added. After stirring at room temperature for 1 h, sulfonated protein was dialyzed against 4 l of 0.1% acetic acid at 4 °C. Dialysis against 5 l buffer was carried out for 4 cycles of 8 h each. The precipitated protein was then collected by centrifugation at 10,000 rpm in GSA rotor at 4 °C for 20 min. To refold the sulfonated protein, the pellet was resuspended in 200 ml refolding buffer (6M guanidine–HCl, 50 mM Tris–HCl, pH 8.0) at room temperature, and then dialysed against 4 l of dialysis buffer (0.9 M Guanidine–HCl, 50 mM Tris–HCl, 5 mM cysteine, 5 mM EDTA, pH 8.0) at 4 °C. The buffer was changed after 6 h, and then dialysis continued for additional 24 h. Next four dialysis cycles of 6 h for each were carried out against trypsinization buffer (50 mM Tris–HCl, 100 mM NaCl, 1 mM $CaCl_2$, pH 8.0). Protein was recovered by centrifugation at 9,000 rpm, 4 °C, for 20 min in GSA rotor, and any insoluble material was discarded.

The refolded GST-proPLA2 fusion protein was activated with 0.0015 mg trypsin per mg fusion protein per ml buffer. Once the PLA2 activity was maximized the pH was adjusted to 4.5 to stop the trypsin reaction. The mixture was then immediately loaded into S-Sepharose column. The protein was eluted with 100 ml gradient of 0 to 500 mM NaCl in 0.1 mM sodium succinate (pH 4.5). The fractions with PLA2 activity were pooled and dialyzed against water at 4 °C. The dialyzed PLA2 fraction was concentrated to 1 ml by lyophilization. It was then injected into preparative C18-HPLC column and eluted with a gradient of solvent B (0.1% trifluoroacetic acid in acetonitrile) with solvent A (0.1% trifluoroacetic acid in H_2O). The fractions with PLA2 activity were pooled together, lyophilized, and purity checked on analytical C4 column.

2.3. Characterization of the interfacial turnover and competitive inhibition

The processive interfacial turnover rate on sonicated DMPM vesicles was measured by pH-stat titration with 1 mM 2-aminopropanediol after adding the enzyme to 0.4 mM DMPM and 40 μg polymyxin B to a 4 ml reaction buffer containing 0.5 mM CaCl2, 1 mM NaCl at pH 8.0 and 24 °C in a nitrogen purged closed atmosphere [4,31,32]. Turnover rate with 2 mM DC_7PC micelles was monitored in 4 ml reaction buffer containing 5 mM $CaCl_2$ and 4 M NaCl at pH 8.0 [28,29]. Under these conditions high salt lowers K_d and increases k^*_{cat}. In both of these assays the observed rate v_o is at the mole fraction of the substrate $X^*_S = 1$. $X_I(50)$* is the mole fraction of the competitive inhibitor MJ33 at which the observed rate decreases by 50% [31].

2.4. Fluorescence measurements

Changes in the tryptophan fluorescence emission spectra and intensity were measured in the ratio mode on SLM-Aminco AB2 in a 1-cm cuvette [9,33] . The slit-widths were 4 nm with excitation at 280. Stirred 1.6 ml buffer for all measurement contained 1 or 2 μM PLA2 in 10 mM Tris, 0.5 mM $CaCl_2$ at pH 8.0 with 20 mM NaCl for the spectral studies. Results with Trp-free W3F mutant

of pig WT show that the contribution of the tyrosines in PLA2 to the emission spectrum and the spectral change is typically less than 2% in the quantum yield or the emission intensity at 333 nm. All fluorescence measurements with bound enzyme were carried out with the nonhydrolyzable substrate analog DTPM, where the bound enzyme is in the E* form in EGTA, and in E*L form in the presence of calcium. For the quenching studies NaCl concentration was 1 mM in order to minimize distortions due to the ionic competition in the electrical double layer of the anionic bilayer vesicles. Stern–Volmer plot was obtained from the successively added total quencher concentration dependence of the emission intensity (F_o/F_q).

2.5. Modification of the Trp-substituent with NBS

Reaction progress for the oxidation of Trp of 0.5 μM PLA2 in 10 mM Tris, pH 8.0 (and other reagents as specified) with 0.2 mM NBS [34] was monitored as the decrease in the fluorescence emission at 340 nm. Under these conditions the rate is not limited by the NBS concentration. Only the halftimes > 10 s are reliable because the mixing time for NBS added to initiate the reaction is about 2 s. Fresh stock solution of NBS (100 mM in tetrahydrofuran containing 0.025% butylated hydroxytoluene as antioxidant) kept in ice could be used for 4 h without significant deterioration.

3. Results

Trp-mutants are constructed by substitution of single Trp on the W3F PLA2 mutant without any Trp residue. As shown in Fig. 1 most of these substitutions (except at 87) are on, at or near the edge of the i-face that makes contact with the interface. Kinetic results show that the mutants with comparable interfacial kinetic and binding parameters are useful for mapping the Trp-microenvironment because the K_d values for the mutants bound to DTPM or $DTSO_4$ interface are not noticeably different. Our strategy for the evaluation of the i-face interactions in terms of the changes associated with the E o E* or ECa to E*L is outlined in Scheme 2. Calcium is obligatorily required for the binding of the substrate to the active site of E* and also for the chemical step [20,35]. Thus titration of E with DTPM vesicles (Fig. 2) in the absence of calcium is for the E to E*, and in the presence of calcium it is for ECa to E*L. K_L^* (for ECa*L or E*L to E*Ca + L*) is 0.03 mole fraction DTPM, and K_{Ca}^{app} for E*L (E*CaL to E* + L* + Ca) is 0.06 mM [35]. Thus, in the presence or absence of calcium the enzyme bound to the DTPM vesicles would be only in the E*L or the E* form, respectively. In both cases the signal saturates at 35 DTPM/E for all mutants although the maximum signal intensity depends on the position of the Trp-substitution.

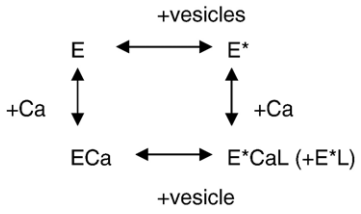

Scheme 2. Relationship between the calcium binding, binding of DTPM (= L) to the occupancy of the active site to form E*L (+E*.Ca.DTPM), and the binding of PLA2 to DTPM vesicles to form E* without the occupancy of the active site.

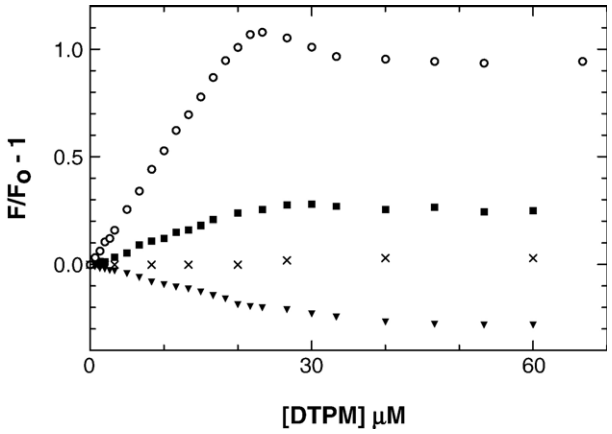

Fig. 2. The change in the normalized Trp-emission intensity at 333 nm (excitation 280 nm) of 1 μM PLA2 as a function of added DTPM concentration corrected for the phospholipid molecules available on the outer surface of the vesicles. From top: (circles) WT (W3), (squares) W3F/L19W, (crosses) W3F, or (triangles) W3F/M20W. The control with W3F shows that the change in the fluorescence emission intensity from tyrosines of PLA2 is negligible. The rising part of the titration curve saturates at about 35 DTPM per enzyme. From these curves the upper limit estimate of K_d is submicromolar that cannot be adequately estimated even with the fit to the quadratic relation based on the consideration of the depletion of the interface on the binding of the enzyme [66].

3.1. Interfacial catalytic turnover by the Trp-mutants of PLA2

Values of the interfacial kinetic parameters for the hydrolysis of DMPM vesicles [32] or DC_7PC micelles [28] by the Trp-mutants are summarized in Table 1. The initial rate with all the enzyme bound to the interface, v_o, is the steady-state interfacial turnover rate by E* via E*S at $X_S^* = 1$ mole fraction [5,6]. It is related to the interfacial substrate binding (K_M^*) and catalytic steps (k_{cat}^*). $X_I(50)^*$, the mole fraction of the competitive inhibitor MJ33 at which the observed interfacial turnover rate is 50% lower, is related to relative affinities of the substrate and MJ33. $X_I(50)^*$ values for the Trp-mutants differ by less than 2-fold which suggests that the relative affinity for MJ33 versus the substrate DMPM or DC_7PC does not change significantly with the Trp-substitutions [5,6,31]. However, $X_I(50)^*$ for the W3F/L31W double mutant relative to the W3F mutant is significantly lower with the DMPM substrate but not with DC_7PC. This is expected if the affinity of the double mutant is lower for DMPM but not for DC_7PC.

The v_o values for the Trp-mutants are between 300 and 6 s^{-1} for DMPM and 600 and 20 s^{-1} for DC_7PC, and for most mutants v_o values for the two substrates change similarly. Compared to the WT v_o for W3F is significantly lower. Results for the mutants #2–4 and #9–13 (Table 1) show that Trp-substitution on the N-terminus (1,10)-helix lowers the rate by another factor of 3. Such modest effects of Trp-substitution on the interfacial catalytic turnover parameters are attributed to the allosteric effects of the i-face interactions [20,36]. As discussed, later interactions of the 1,10-helix in the active site pocket may mediate allosteric interactions. Kinetic effects on v_o with a modest discrimination of DMPM versus DC_7PC are also apparent with the substitutions and deletions on the N-terminus helix of bovine [29,36] and pig [1,23,37,38] PLA2.

3.2. Tight binding of PLA2 is not influenced by the Trp-substitutions

Interpretation of the kinetic results in Table 1 is based on the assumption that during the processive interfacial turnover PLA2 remains tightly bound to the substrate interface [4,5]. This is shown by the results (not shown) that all Trp-mutants showed a first-order reaction progress on DMPM vesicles [4] and the extent of hydrolysis per enzyme is the same with all the mutants. Spectroscopic evidence for the tight binding of Trp-mutants to DTPM vesicles is shown in Fig. 2. The control with W3F shows that the signal from the Trp-substitution is 30- to 50-fold larger than with the tyrosines together. From the steep dependence of the change in the Trp-fluorescence emission intensity with DTPM concentration estimated K_d for the binding of the mutants is submicromolar. With all Trp-mutants the spectral change saturates at 30 ± 5 DTPM per enzyme molecule. The surprising result in Fig. 2 is that the magnitude and the direction of the signal change depend on the position of the Trp-substituent. As discussed later such differences are due to the differences in the Trp environments in the E and E*L forms. Also insignificant effect of substitution of cationic residues 6 and 10 (Table 1) on the processive turnover is consistent with a minor role of Coulombic interactions [39]. Together, the kinetic and spectroscopic results show that the tight binding of PLA2 to the DMPM or DC_7PC interface [3,4,40] is not influenced by Trp-substitutions. Note that the kinetic results obtained under other assay conditions [41,42], where the binding of the enzyme to the interface is not tight, would be influenced by modest changes in K_d.

Table 2
Relative quantum yield[a] of Trp-mutants and complexes

PLA2	Ca (mM)	QE	QE*(DTPM)	QE*(DTSO4)
3W(WT)	−	1.10 (=E)	1.76 (= E*)	1.21 (=E*)
	+	1.0 (+ECa)	2.72 (=E*L)	1.40 (=E*L)
1W	−	0.89	0.93	
	+	0.84	0.92	
2W	−	0.70	0.72	
	+	0.79	0.67	
6W	−	2.34	2.38	2.84
	+	2.39	2.38	2.67
10W	−	1.25	0.75	1.09
	+	1.22	0.63	1.09
19W	−	1.32	1.40	1.60
	+	1.24	1.65	1.98
20W	−	1.60	1.65	2.10
	+	1.56	1.50	2.01
31W	−	1.28	0.79	–
	+	1.24	0.74	–
53W	−	1.54	1.57	1.52
	+	1.55	1.46	1.46
56W	−	1.86	1.88	3.0
	+	1.93	3.13	3.66
63W	−	1.50	1.50	1.30
	+	1.35	1.80	2.28
87W	−	1.75	1.75	1.66
	+	1.80	1.84	1.68
117W	−	1.75	1.54	2.95
	+	1.38	0.63	2.98

[a] In the aqueous phase the quantum yield (for the excitation at 280 nm) of the ECa form of WT PLA2 is 0.11 compared to 0.3 for N-acetyltrytophan-amide (NATA). Uncertainty in the relative quantum yield is 20% including the uncertainties in the measurement of the protein concentrations. Spectra for 1 μM mutant solutions without or with 0.2 mM DTPM or $DTSO_4$ vesicles were obtained at the same sensitivity settings and the control for the buffer is subtracted from the area integral for the emission from 300 to 400 nm. Spectra in the absence of calcium (marked with −) were obtained in 1 mM EGTA + 1 mM EDTA, and those marked with + were obtained with 20 mM calcium for the ECa form and 0.5 mM calcium for the E*L form (Scheme 2).

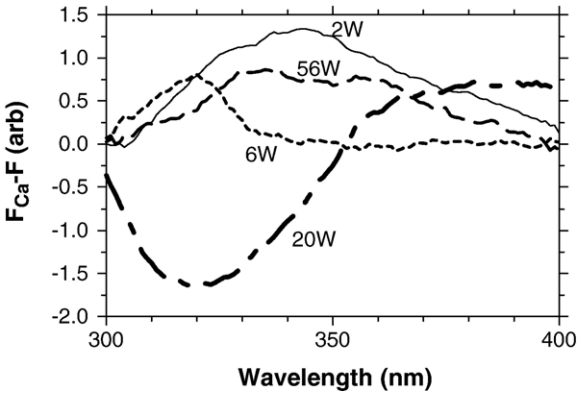

Fig. 3. Change in the emission spectrum of (continuous line) 2W, (dashed line) 6W, (dot-dash) 20W, and (broken line) 56W mutant on the addition of 20 mM calcium. Ordinate is an arbitrary scale at the same protein concentration and instrument settings. The peak or trough at 320 nm in the difference spectrum from 6W or 20W is unlikely to be due to the perturbation of a tyrosine because controls with W3F do not show such a change.

3.3. Spectral Difference between the E and E.Ca forms

Relative quantum yields of the E, ECa, E* and E*L complexes (Scheme 2) of Trp-mutants are compared in Table 2. About 3-fold range of these values is attributed to the change in the local environment. It is not trivial to assign specific interactions responsible for such differences because the fluorescence emission change is the sum total of the photon, electron and proton transfer reactions in the ground and excited states of the fluorophore. Therefore, the changes are only qualitatively interpreted. Detailed spectral analysis of the spectral emission maximum and the center of mass, as well as the life time measurements, were not carried out. For example, the difference spectra in Fig. 3 show that effect of the calcium binding is qualitatively different for the Trp-substituent at 2, 6, 20 or 53. Changes in quantum yield associated with the calcium binding are summarized in column 3 of Table 2. The results for 117W were obtained by subtracting the corresponding changes in 3W from the changes observed with 3W/117W double mutant. These results show that the calcium binding to the E form has a modest effect on the Trp environment. Typically, the calcium induced spectral change is small, however, such changes are detected by the Trp probe located in certain positions that are > 10 Å away from the calcium bond to the (27–32)-loop [43,44]. For example, the calcium binding influences the emission from 53W and 56W on the 41–57 helix containing the catalytic residue H48. This effect may be mediated via D49 whose side chain carboxylate provides two ligands for the

calcium binding. Also, note that 20W is significantly perturbed on the calcium binding, but the emission from 19W or 31W is not. These results suggest that the quantum yield changes associated with calcium binding are modest specific intramolecular changes.

3.4. Spectral changes due to E* and E*L formation

Relative quantum yields of E* and E*L complexes of the Trp-mutants are summarized in Table 2. Results in column 4 are for E* or E*L on DTPM vesicles and in column 5 for E* or E*L on $DTSO_4$ vesicles. The key result is that magnitude and direction of the change in the quantum yield depend on the position of the Trp-substituent. For example, the relative quantum yield from Trp-3 in WT is 1.1 for E, 1.0 for ECa, 1.76 for E*, and 2.72 for E*L on DTPM. The quantum yield of the E*L of 3W, 19W, 56, or 63W on DTPM is higher and the emission maximum is blue-shifted by about 10 nm. On the other hand, the quantum yield of the E*L form is lower for Trp at 2, 10, 53 or 117 with a red shift of 5 to 12 nm in the emission maximum. The quantum yield changes little for Trp at 1, 6 or 20.

Note that 87W on the surface away from the i-face does not show a significant perturbation neither on the binding of calcium, nor with the formation of E* or E*L complex on DTPM or $DTSO_4$ interface. However, other effects show spectral contributions of the local environment. As shown in Fig. 4, the difference spectra for E*-E and E*L-ECa of the Trp-19 mutant are different on the DTPM versus $DTSO_4$ vesicles. Other Trp-mutants also show such differences (columns 4 and 5 in Table 2). Since Trp-mutants bind tightly to DTPM and $DTSO_4$ anionic interfaces, such spectral differences imply a role for the short-range interactions with the anionic head group. Such E*L-ECa spectral differences are not expected to be very different if electrostatic interactions dominate the interactions along the i-face, or if the spectral changes were only due to a change in the polarity of the Trp-environment.

The E*L-ECa difference spectra in Fig. 5 show the spectral effects of the neighboring substituents. For example, the Trp-3

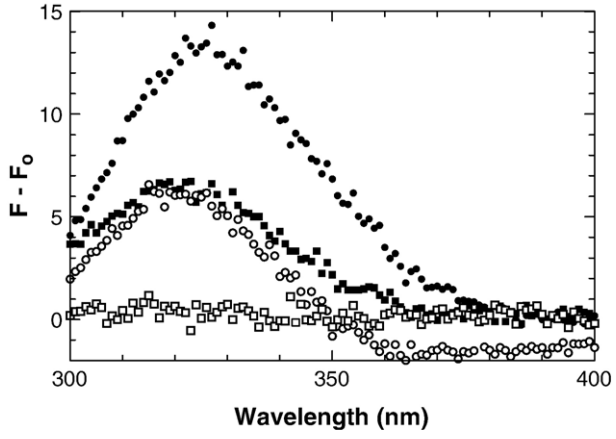

Fig. 4. Change in the emission spectrum of W3F/L19W on the addition of saturating (circles) $DTSO_4$ or (squares) DTPM in the presence of (filled symbols) 0.5 mM calcium or (unfilled symbols) 1 mM EGTA + 1 mM EDTA.

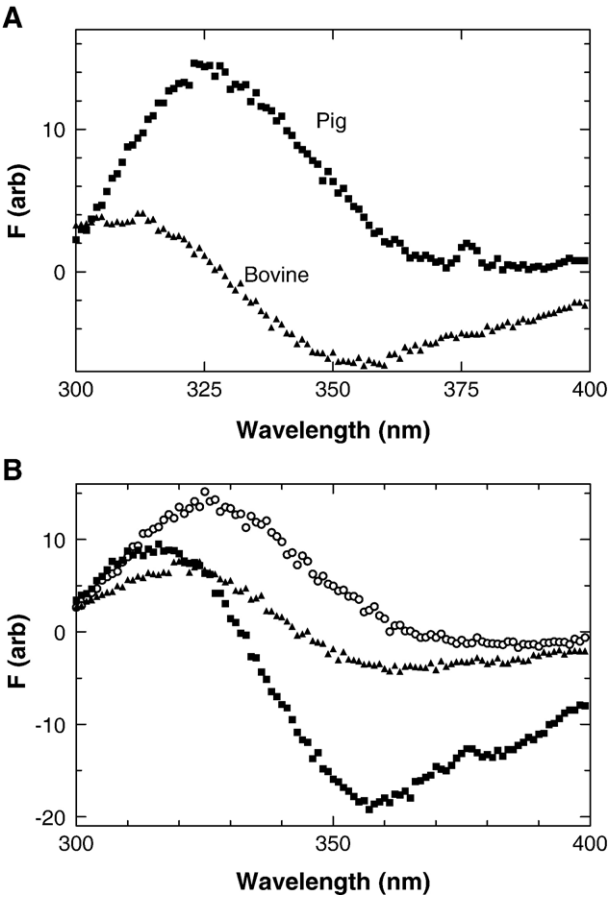

Fig. 5. The change in the spectrum of PLA2 and mutants on the binding to DTPM in the presence of calcium: [A] pig and bovine WT, both of which contain Trp-3, or [B] from bottom (squares) N117W, (triangles) D119Y/117W, or (circles) K116Y/D119Y/117W. The spectral changes from W3 have been subtracted from the spectra of the mutants. files FfiveApig-bov diff.pzm, FfiveB-117W-diffspectra-set.4B.pzm.

spectral change from pig PLA2 is different than that from bovine PLA2 (Fig. 5A). These proteins have 70% sequence homology [1], and their interfacial catalytic behavior and the NMR and crystal structures are also virtually indistinguishable [15,19,22,45,46]. Similarly, effects of the Y116 and Y116/Y119A substitutions on the emission from Trp-117 in pig PLA2 is shown in Fig. 5B. These results show that such large differences could arise from a single residue substitution.

3.5. Accessibility of the Trp-substituents to aqueous quenchers

Accessibility of the Trp-substituent on the i-face to a dynamic collisional quencher in the aqueous phase is expected to decrease significantly with the formation of E* or E*L. As shown in Fig. 6, the quencher concentration dependence of the emission from Trp-3 is significantly different for the E versus the E*L of PLA2. Linear Stern–Volmer plots are consistent with the dynamic collisional quenching mechanism. Qualitatively similar results are obtained from three different quenchers: Uncharged succinimide, anionic iodide, and cationic cesium. The quencher concentrations for 50% quenching obtained from such plots are summarized in Table 3 as the Q_{50} values for the E,

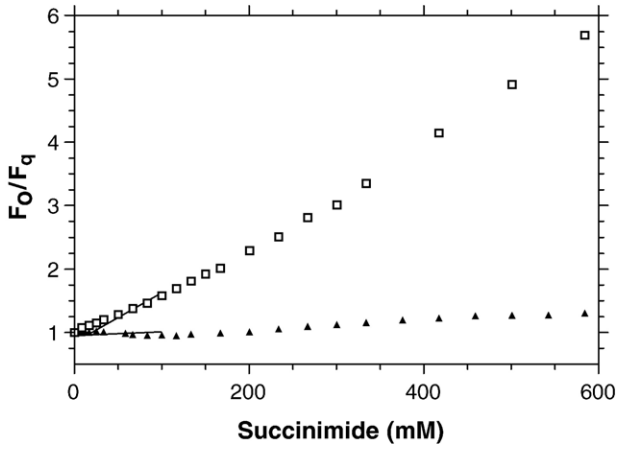

Fig. 6. Stern–Volmer plots (with F_o/F_q as the ordinate) for the quenching by succinimide of WT PLA2 (1 μM) in the (squares) *E* or (triangles) *E** form on DTPM vesicles.

ECa, E* and E*L forms of the Trp-mutants. The Stern–Volmer constant is reciprocal of Q_{50}, however in consideration of uncertainty about the quenching mechanism (see below), we have not expressed the quenching results as the Stern–Volmer quenching constant. The Q_{50} values increase if Trp is more shielded. As expected for Trp localized on the protein surface, Q_{50} values for the E form of all the Trp-mutants are in the 100 to 200 mM range for succinimide compared to 70 mM for N-acetyltryptophan-amide (NATA) in the aqueous phase. In contrast, Q_{50} values for the E* and E*L form of the Trp-mutants are in the 130 to 1800 mM range. Q_{50} changes little for 31W, 53W and 87W mutants, and increases 3-fold or more for 3W, 63W and 117W. In addition to the consideration of the shielding effects and the solvent interactions in the Trp-environment [39], for a detailed quantitative interpretation of the Q_{50} values, it is also necessary to consider the changes in the orientation and relaxation of the neighboring substituents. Since the relaxation behavior of the Trp-3 in PLA2 is far too complex [33] we did not to carry out detailed physical analyses.

For some of the Trp-substituents, the non-linearity in the Stern–Volmer plots for the quenching by cationic cesium or anionic iodide is significant. For example, with iodide a downward curvature is seen with the E form of 6W suggesting that in the E form iodide binds near 6W (Fig. 7A). Such curvature could result if the quencher bound to the complex is more efficient [47,48] which is consistent with the possibility that the iodide binding site could be in the cluster of the three anion-binding sites (Fig. 1) in the anion-assisted dimer structure [22,23,49,50]. As expected, the plot for the E*L form of 6W is linear presumably because the anion binding sites on the enzyme are occupied by the interfacial anionic groups. Similarly, in Fig. 7B with cesium the downward curvature is seen for the E*L form of 20W suggesting that Cs is bound close to 20W in the E*L form on the anionic DTPM vesicles. Also, as summarized in Table 3, quenching with cesium is not very efficient: Q_{50} of 400 to 800 mM for the E form of most mutants, and somewhat more for 1W, 2W, 19W, and 117W. Our interpretation is that the cationic electrical double layer due to

Table 3
Q_{50} values[a] for ECa and E*L(DTPM) forms of PLA2 mutants

	Succinimide		Iodide		Cesium	
Mutant	ECa	E*L	ECa	E*L	ECa	E*L
WT/3W	128	1700	180*	1100	800	2300
-6M	190	>1000			900	>1500
-10M	210	>1000			840	>1200
-6,10M	145	585			800	>1200
-117W	110	450	190	480	800	1200
-117W/119Y	160	470			1000	>1200
117W/116,119Y	165	495			>1200	>1200
W3F-1W	205	500			>1000	>1500
-2W	170	350			>1200	>1500
-6W	200	500	100*	395	1200	1900
-10W	140	360	200*	350	370	1200
-19W	200	380	210	520	1000	1100
-20W	200	400			500*	260*
-31W	80	130				
-53W	80	200	240	580	480	600
-56W	150	360	330	690	740	1100
-63W	115	590			550	1200
-87W	90	220			450	540

[a] Uncertainty in the Q_{50} values is 10% unless the Stern–Volmer plot is significantly biphasic (marked with *).

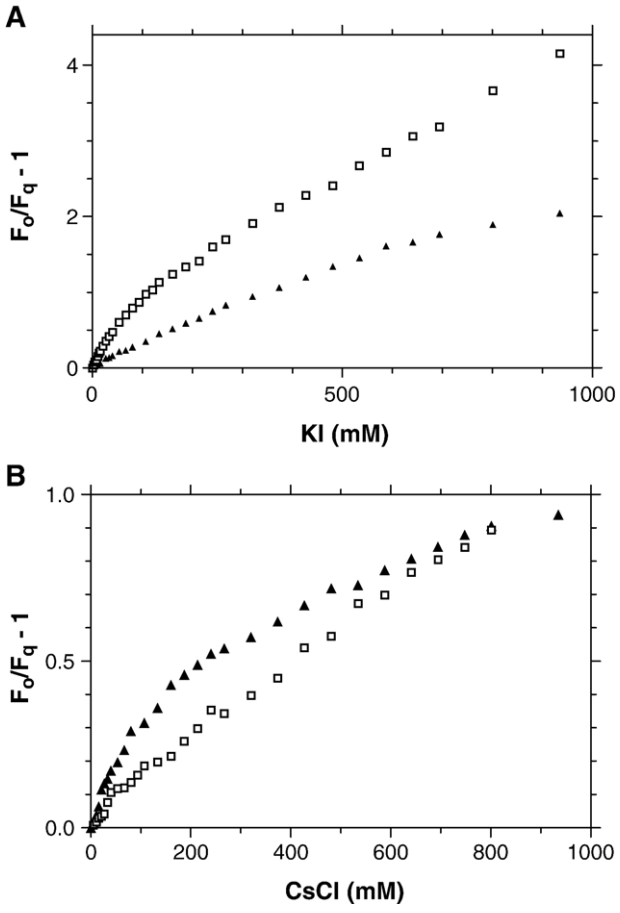

Fig. 7. (A and B) Stern–Volmer plots (with $F_o/F_q - 1$ as the ordinate) for quenching of (A) W3F/R6W with KI or (B) W3F/M20W with CsCl for the (squares) free E form or (triangles) E*L form bound to 100 μM DTPM vesicles in 0.5 mM $CaCl_2$.

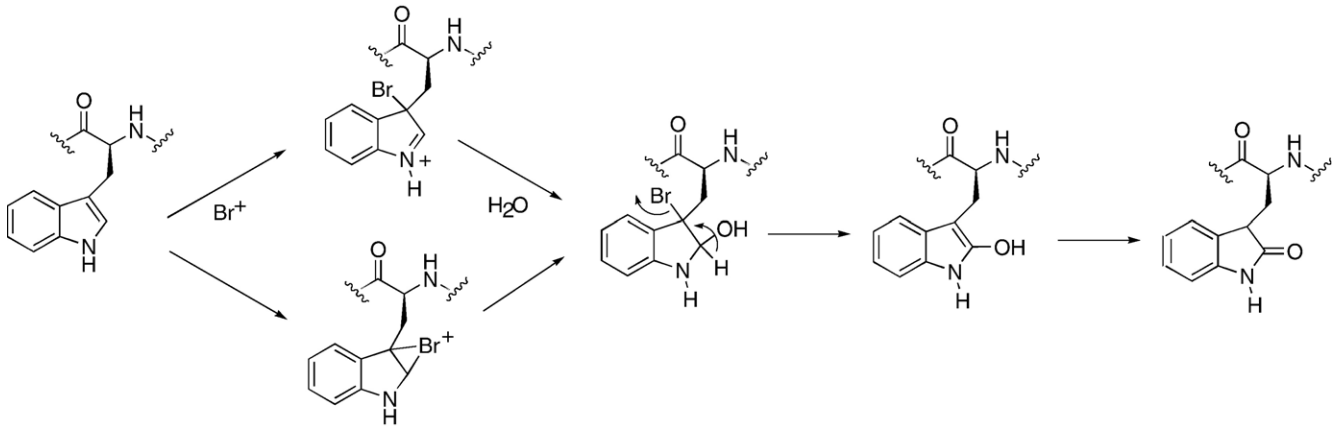

Scheme 3. Suggested mechanism of oxidation of Trp by NBS where the initial attack of bromonium ion (derived from NBS or HOBr or $[H_2OBr]^+$) is followed by attack of water to give non-fluorescent oxotryptophan. Rate in the slower second step is limited by the water concentration in the Trp environment.

the 12 cationic residues on the surface of PLA2 electrostatically shields Trp from cesium. Qualitatively, the quenching results in Table 3 suggest that the effects of the electrical double layer [51,52] on the protein and the bilayer interface are weaker than those of the short-range interactions along the i-face. Together, these results suggest complex collisional quenching behavior for the Trp-substituent on the i-face of PLA2 in the E* or E*L form. Some of these difficulties are circumvented by results described below where the rate of Trp-oxidation is limited not as much by NBS accessibility but by the hydration step.

3.6. Covalent modification of the Trp-substituents with NBS

Oxidation of tryptophan with N-bromosuccinimide yields nonfluorescent 2-oxotryptophan [34]. As suggested in Scheme 3 at neutral pH the initial attack by bromonium ion is followed by attack with water. These two steps are kinetically resolved under certain conditions [53]. As shown in Fig. 8A the rate of reaction of octyltryptophan with NBS is noticeably slower in the presence of DTPM vesicles. Also the rate of oxidation of bound octyltryptophan is slower in D_2O than in the H_2O. As summarized in Fig. 8B, dependence of the observed rate constant on the mole fraction of D_2O is almost linear and the H_2O/D_2O isotope effect is 2. Together, these results suggest that

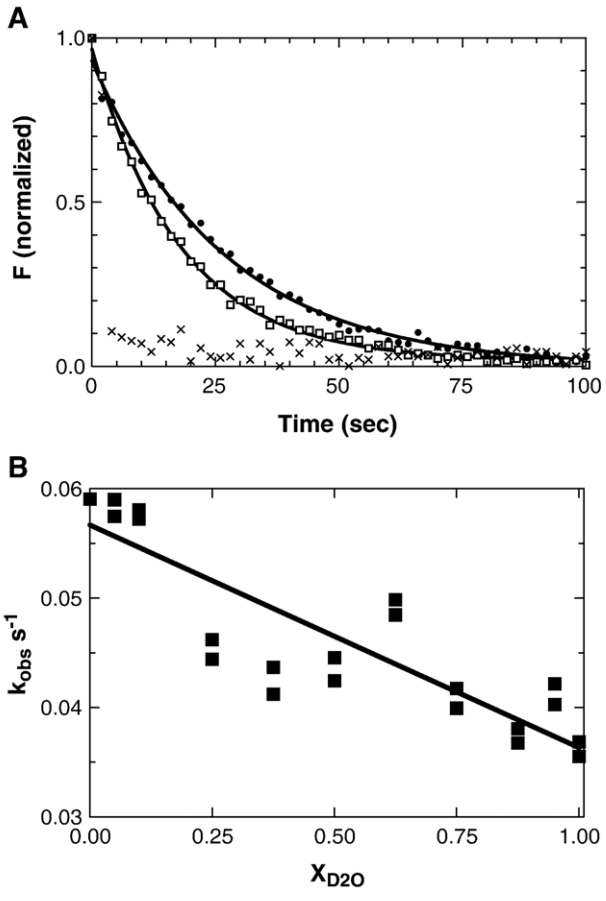

Fig. 8. [A] Reaction progress for the reaction of 0.2 mM NBS with 0.5 μM octyltryptophan (crosses) alone in H_2O, or (squares) with 0.4 mM DTPM in H_2O or (circles) in D_2O buffer (10 mM Tris at pH 8.0). Ordinates are normalized. The mixing time is < 5 s. Fit for single exponential decay gives halftime of 11.5 s in H_2O and 20 s in D_2O. [B] Values of the rate constant for the slower step for the modification of 1 μM PLA2 with 0.2 mM NBS as a function of the mole fraction of D_2O in the buffer.

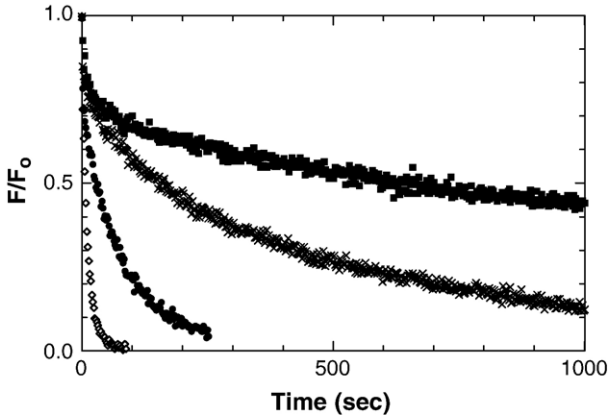

Fig. 9. Time course of the NBS induced quenching of the normalized fluorescence of 3W-PLA2 in (open diamonds) E or (crosses) E* form on 0.2 mM DTPM vesicles in H_2O buffer, and for the (filled circles) E or (filled squares) E* forms in D_2O buffer (1 mM EGTA + 1 mM EDTA, 10 mM Tris at pH 8.0 or 7.6 in D_2O).

the rate-limiting step in the oxidative quenching by NBS under the water-limiting conditions is likely to be the attack by water.

The rate of the reaction of NBS with most Trp-mutants is significantly lower for E* and E*L forms of PLA2. As shown in Fig. 9, the time course of the decrease in the Trp fluorescence of the E form of PLA2 on the addition of NBS is biphasic: Following the initial rapid decrease, further quenching occurs with halftime of >20 s in H_2O and noticeably longer in D_2O. As also shown in Fig. 9, the rate of reaction with NBS is considerably slower for the E* form and the H_2O/D_2O effect on the rate is also clearly apparent. For the E* or E*L form of the mutants with Trp on the i-face the apparent H_2O/D_2O effect in the second step of the reaction of NBS remains about 2 (results not shown). This is expected if the attack by water remains the rate-limiting step.

Table 4
Half-times (t_1 and t_2 in s) for the oxidation of Trp-mutants by NBS

Trp at Form		t_1/a_1	t_2/a_2
1W	E*L	14/0.2	> 1000
	E*	6/0.7	270/0.3
	ECa	3/0.34	22/0.58
	E	5/0.6	46/0.3
2W	E*L	3/0.36	50/0.3
	E*	3/0.63	70/0.32
	ECa	3/1	
	E	4/1	
3W	E*L	130/0.65	> 1000
	E*	51/0.18	420/0.48
	ECa	5/0.93	32/0.13
	E	8/0.98	
pro-	E*L	6/0.9	
	E*	10/0.9	
	ECa	13/0.9	
6W	E*L	2/0.35	130/0.4
	E*	1/0.1	140/0.9
	ECa	3/1	
	E	3/1	
10W	E*L	1.4/0.3	25/0.32
	E*	4.6/0.45	15/0.52
	ECa	2.5/0.38	16/0.52
	E	1/0.37	12/0.6
19W	E*L	10/0.63	202/0.27
	E*	5/0.53	82/0.23
	ECa	11/0.95	
	E	12/0.92	
20W	E*L	3/0.63	30/0.29
	E*	1.5/0.39	15/0.56
	ECa	6/0.60	33/0.4
	E	1/0.22	15/0.76
53W	E*L	19/0.15	> 1000
	E*	12/0.35	> 1000
	ECa	6/0.95	
	E	4/0.95	
56W	E*L	5/3	76/0.7
	E*	3.4/0.9	
	ECa	2/1	
	E	2/1	
63W	E*L	0.6/0.3	13/0.48
	E*	1.6(0.84)	18/0.12
	ECa	8/0.69	17/0.36
	E	9/1	
87W	E*L	3/0.98	
	E*	2/1	
	ECa	5/0.95	
	E	2/0.95	

[a]Values of the half-time (s) and the fractional amplitude change (t_1/a_1 and t_2/a_2) are for the first and second phase of the fluorescence decrease after the addition of 0.2 mM NBS to 1 μM Trp-mutant at pH 8.0 (20 mM Tris and 10 mM NaCl) with 0.2 mM DTPM for the E* and E*L forms, and with 0.5 mM $CaCl_2$ for the ECa and E*L forms.

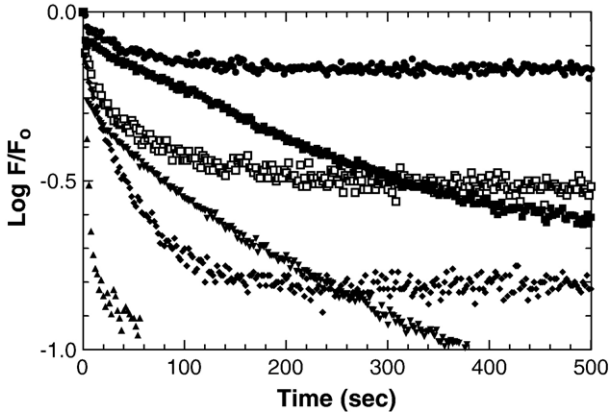

Fig. 10. Reaction progress (on a logarithmic ordinate, i.e., the fluorescence is 90% quenched at − 1) for the reaction of 0.2 mM NBS with the E*L form (0.5 mM $CaCl_2$ and 0.2 mM DTPM in H2O buffer) of PLA2 mutant with (from the fastest or bottom (triangles) 87W, (diamonds) 10 W, (inverted triangles) 56W, (unfilled squares) 2W, (filled squares) 3W, and (top curve, diamonds) 53W. (file Ften-NBS-WTELCa-H2O).

The half-times for the reaction of NBS with E and ECa forms of the Trp mutants are compared in Table 4. In all cases, the halftime for the initial decrease is < 10 s during which 15 to 50% of the florescence is quenched. The halftime for the second step is < 30 s with the E and ECa forms of virtually all the mutants. These results are consistent with the surface localization of the Trp-substituent, and also that the bromo-tryptophan intermediate remains readily accessible to the water reagent in the second step. As shown in Fig. 10 and summarized in Table 4 the time course for the reaction of NBS with the E* or E*L forms of the mutants depends on the position of Trp. The halftime for the initial decrease is typically < 20 s for all the mutants during which the signal decreases by 20–70% (fractional values given in the parenthesis). The second step is considerably slower for the E* and E*L forms of certain mutants. For example, accessibility of bromo-intermediate of W1, W3 or W53 to reacting water is most shielded, and a more modest shielding of 2W, 6W and 19W. Together, these results show that the accessibility of reagent water for the NBS oxidation of Trp substituent NBS depends on its localization along the i-face, and possibly also on the occupancy of the active site.

4. Discussion

The active site of PLA2 is structurally and functionally distinct that the i-face along which the enzyme binds to the interface [1,54]. Also binding of the enzyme along the i-face to the substrate interface is a distinctly different event than the binding of the substrate in the interface to the active site of the bound enzyme (Scheme 1 and 2). Both of these steps have characteristic microscopic variables and constants, and the

structural, functional and thermodynamic constraints are different. Structural significance of such events is beginning to converge into a viable model shown in Fig. 1. Since originally proposed in 1991, this model of the i-face has served well to rationalize virtually all aspects of interfacial kinetic phenomena [5,6,18,29,44,46]. It has also provided a basis for the analytical descriptions with predictive value [4–6,12]. Significance of results in this paper is developed below.

Current model of the i-face [2] emerged from the key result that during the processive interfacial turnover PLA2 binds tightly to the anionic interface [3,4]. Wide ranging kinetic, spectroscopic and crystallographic results have provided additional insights [5,6,21]. For example, the tight binding of E* and E*L is accompanied by desolvation of the i-face in contact with about 30 molecules of phospholipid per PLA2 at the anionic interface [4,8,55–57]. Since binding of PLA2 does not disrupt bilayer, the i-face is unlikely to penetrate into the bilayer. Although tight binding is observed only with anionic interface, Coulombic interactions contribute < 2 kcal/mole to the stability of E*. Also, about 22 (Hill number) monodisperse alkylsulfate molecules cooperatively bind in three discrete steps, and such binding is perturbed if the active site residues are mutated [39,58]. Additional support for this model comes from the X-ray structures of the anion-assisted homodimer of PLA2 [21–23,50] where the contact surface of the two subunits is virtually the same as the originally suggested i-face. The contact surface brings the two subunits within < 5 Å with five coplanar anion sulfate or phosphate anion binding sites. Although inconsistent with our results, some results have been interpreted to suggest that PLA2 penetrates into the bilayer [1,54,59,60], or that electrostatic interactions dominate the interaction [44].

4.1. Rationale for the Trp-substitution at the i-face

Results in this paper provide insights into the nature of the tight binding interactions of PLA2 with anionic vesicles. Trp-mutants of PLA2 are useful probes because the substitutions are benign with respect to catalytic activity (Table 1). Also, Trp-substitutions do not significantly influence the tight interfacial binding (Fig. 2) or the processive catalytic turnover rate (Table 1). The processive behavior is also consistent with apparent K_d of < 10^{-12} M on the anionic vesicles [4,26]. Modest effects of substituents on tight binding would not show up in these measurements. For example, a change of about 2 kcal/mole in the binding energy would have a significant effect only if $K_d > 1$ μM. However, modest changes in i-face interactions may influence the catalytic turnover rates [20], interface preference [29], and allosteric effect of the interface [13,29] which together may account for modest effects on v_o (Table 1). By other methods, we are exploring thermodynamic, structural and functional reciprocity of the coupling between the i-face and the active site events.

Effects of the substitutions on the N-terminus are of particular interest. It is part of the i-face and the 1,10-helix also becomes more ordered as the active site is occupied. In the crystal structures of PLA2 cocrystallized with the substrate mimics the *sn*-2-chain makes van der Waal contact with residue 5 at C_3–C_4 and with residue 2 at C_8–C_9. The C_8–C_{11} of the *sn*-1-chain is near L31 [10,15,19,22,23,44,50]. Also, R6 and K10 provide ligands for the anion binding along the i-face. The NMR evidence shows that the residues 1, 2 and 3 are more helically ordered in the zwitterionic micellar complex of the enzyme with occupied active site [16]. Based on such considerations, we suggest that the short-range anion binding to ligands on i-face mediate allosteric activation of E* and E*L. One possibility is that the H-bonding network, involving several residues spanning from α-NH_2 at the N-terminus to the catalytic site involving D99-H48 and the calcium binding site involving D49 [1,6,20,39,58], mediates the allosteric k^*_{cat}-activation.

4.2. Microenvironment of the Trp substituents

Fluorescence emission from a single Trp on the surface of a protein is influenced by several factors [47,48] including heterogeneity of the Trp environment due to water accessibility, relative population of the indole rotamers, as well as the amide, carboxyl, imidazole (His), phenol (Tyr), thioether (Met) and disulfide (Cys) groups within 5 Å [61–64]. Such effects provide a sensitive measure of the short-range changes in the Trp-environment seen in the difference spectra, however, make it nearly impossible to assign specific structural change. Spectral changes associated with the formation of ECa, E* and E*L forms on DTPM and $DTSO_4$ (Table 2) suggest that both the protein residues and the groups at the interface influence the change. Result that 87W is not perturbed under most conditions is consistent with the fact that it is neither on the i-face nor in the active site or the calcium binding site. Calcium binding has modest effect on the emission from certain mutants. However, significant spectral change is seen with the formation of E* and E*L of most other mutants where the Trp-substituent is on the i-face. These results are also consistent with our earlier result that the cation binding or the occupancy of the active site is not obligatory for the binding of the enzyme to the interface [35, 65]. Together, these results show that Trp-microenvironment is markedly sensitive to the short range interactions along the i-face, however there is no reliable way to interpret the structural origin of such effects.

4.3. Drive for the i-face Interactions

Results in this paper provide a low-resolution map of the i-face of PLA2, i.e. only the Trp-substituents at the putative i-face are spectrally perturbed. Desolvation of the contact of the i-face with the interface [8,9] is expected to facilitate the substrate accessibility by E* for the processive interfacial turnover [3–6]. Also short-range interactions in the vicinity of the Trp-substituents on the desolvated i-face may be responsible for the differences in the fluorescence emission (Table 2), as well as for the differences in the quencher and the water accessibility in the reaction of NBS with the Trp-substituents in the E* and E*L complexes.

Desolvation of the i-face triggered by the short-range specific binding of the anionic head groups to specific protein ligands on the i-face could provide much of the free energy for the tight binding [39]. Our estimate is that the Coulombic (electrostatic) contribution to the interactions along the i-face is less than

− 2 kcal/mole, and a large part (> 10 kcal/mole) of the binding energy comes from the short range specific ion binding through the protein ligands [21,22,39]. Short-range interactions of the head groups with several protein ligands on the i-face also account for the cooperative binding of the monodisperse amphiphiles where the electrostatic contribution from the head group is < 2 kcal/mole [39]. Thus desolvation of the contact region would result as the water ligands are replaced by ligands from the protein and the amphiphile head group. Our view [2,39] is that the enthalpy driven ligand substitution interactions over 3 to 3.5 Å could also promote hydrophobic effect by removing unfavorable contacts with bulk water. This model does not require energetically unfavorable reorganization of the interface due to its penetration in hydrophobic region of the bilayer.

4.4. Solvation environment for the oxidation with NBS.

Structurally NBS is a less polar analog of the dynamic quencher succinimide. The kinetics of modification of the Trp-mutants by NBS is informative because the second phase of the reaction appears to be limited by accessibility to reagent water in E* and E*L (Table 4). The rapid initial reaction suggests that NBS, or HOBr (Scheme 3) or some related specie, rapidly penetrates the i-face contact in E* or E*L. This step is followed by the rate limiting reaction of the intermediate with water. Trp-87 in E* and E*L is not shielded, whereas Trp at most other positions is shielded to differing degrees. Thus, accessibility to water may be different at different locations along the i-face in the E* and E*L complexes. Further interpretation of these results must await a better understanding of the secondary structural effects that determine the magnitude of t_2. Such contributions may come from the changes in the local pH, polarity, steric and conformational effects that distinguish the E* and E*L complexes and the intermediates between the E and E* step.

To recapitulate, catalytic and spectral properties of the Trp-mutants are in general accord with the current model of the i-face of PLA2. However, difference between the desolvation of the i-face of the E* and E*L forms was not anticipated. Such differences may be related to the coupling of the i-face and active site events [5,6,12,13]. Resulting changes in the hydration and H-bonding network may follow from the K_S^*- and k_{cat}^*-allosteric effects of the i-face interactions [5,12,13,28]. It is also of interest that the reactivity of 53W and 56W with NBS is noticeably different in the E and E*L forms. As a basis for the allosteric k_{cat}^*-activation, it could be related to the changes in the catalytic His-48 and the calcium binding ligands of Asp-49 located on the 41–57 helix. If so, additional Trp-mutants could provide useful information about the sub-states formed by binding of amphiphiles to the i-face [39] and also about the role of the residues of the H-bonding network in the allosteric activation of PLA2 [1,58].

Acknowledgments

We thank Professor Joseph Fox for suggesting the mechanism outlined in Scheme 3. This research was funded by PHS (GM-29703 to MKJ).

References

[1] H.M. Verheij, A.J. Slotboom, G.H. de Haas, Structure and function of phospholipase A2, Rev. Physiol., Biochem. Pharmacol. 91 (1981) 91–203.
[2] F. Ramirez, M.K. Jain, Phospholipase A2 at the bilayer interface, Proteins: Struct., Funct., Genet. 9 (1991) 229–239.
[3] M.K. Jain, J. Rogers, D.V. Jahagirdar, J.F. Marecek, F. Ramirez, Kinetics of interfacial catalysis by phospholipase A2 in intravesicle scooting mode, and heterofusion of anionic and zwitterionic vesicles, Biochim. Biophys. Acta 860 (1986) 435–447.
[4] O.G. Berg, B.Z. Yu, J. Rogers, M.K. Jain, Interfacial catalysis by phospholipase A2: determination of the interfacial kinetic rate constants, Biochemistry 30 (1991) 7283–7297.
[5] O.G. Berg, M.K. Jain, Interfacial Enzyme Kinetics, Wiley, London, 2002.
[6] O.G. Berg, M.H. Gelb, M.D. Tsai, M.K. Jain, Interfacial enzymology: the secreted phospholipase A2-paradigm, Chem. Rev. 101 (2001) 2613–2654.
[7] B.Z. Yu, O.G. Berg, M.K. Jain, Hydrolysis of monodisperse phosphatidylcholines by phospholipase A2 occurs on vessel walls and air bubbles, Biochemistry 38 (1999) 10449–10456.
[8] M.K. Jain, W.L. Vaz, Dehydration of the lipid–protein microinterface on binding of phospholipase A2 to lipid bilayers, Biochim. Biophys. Acta 905 (1987) 1–8.
[9] M.K. Jain, B.P. Maliwal, G.H. DeHaas, A.J. Slotboom, Anchoring of phospholipase A2: the effect of anions and deuterated water, and the role of N-terminus region, Biochim. Biophys. Acta 860 (1986) 448–461.
[10] Y.H. Pan, B.Z. Yu, A.G. Singer, F. Ghomashchi, G. Lambeau, M.H. Gelb, M.K. Jain, B.J. Bahnson, Crystal structure of human group X secreted phospholipase A2. Electrostatically neutral interfacial surface targets zwitterionic membranes, J. Biol. Chem. 277 (2002) 29086–29093.
[11] J. Rogers, B.Z. Yu, M.D. Tsai, O.G. Berg, M.K. Jain, Cationic residues 53 and 56 control the anion-induced interfacial k*cat activation of pancreatic phospholipase A2, Biochemistry 37 (1998) 9549–9556.
[12] M.K. Jain, B.Z. Yu, O.G. Berg, Relationship of interfacial equilibria to interfacial activation of phospholipase A2 [published erratum appears in Biochemistry 1994 Jul 19;33(28):8618], Biochemistry 32 (1993) 11319–11329.
[13] B.Z. Yu, M.J. Poi, U.A. Ramagopal, R. Jain, S. Ramakumar, O.G. Berg, M.D. Tsai, K. Sekar, M.K. Jain, Structural basis of the anionic interface preference and k_{cat}^* activation of pancreatic phospholipase A2, Biochemistry 39 (2000) 12312–12323.
[14] B.Z. Yu, T.E. Polenova, M.K. Jain, O.G. Berg, Premicellar complexes of sphingomyelinase mediate enzyme exchange for the stationary phase turnover, Biochim. Biophys. Acta 1712 (2005) 137–151.
[15] M.M. Thunnissen, E. Ab, K.H. Kalk, J. Drenth, B.W. Dijkstra, O.P. Kuipers, R. Dijkman, G.H. de Haas, H.M. Verheij, X-ray structure of phospholipase A2 complexed with a substrate-derived inhibitor, Nature 347 (1990) 689–691.
[16] B. van den Berg, M. Tessari, R. Boelens, R. Dijkman, R. Kaptein, G.H. de Haas, H.M. Verheij, Solution structure of porcine pancreatic phospholipase A2 complexed with micelles and a competitive inhibitor, J. Biomol. NMR 5 (1995) 110–121.
[17] D.L. Scott, Z. Otwinowski, M.H. Gelb, P.B. Sigler, Crystal structure of bee-venom phospholipase A2 in a complex with a transition-state analogue [published erratum appears in Science 1991 May 10;252(5007):764], Science 250 (1990) 1563–1566.
[18] C. Yuan, I.-J. Byeon, Y. Li, M.-D. Tsai, Structural analysis of phospholipase A2 from functional perspective. 1. Functionally relevant solution structure and roles of the hydrogen-bonding network, Biochemistry 38 (1999) 2909–2918.
[19] K. Sekar, S. Eswaramoorthy, M.K. Jain, M. Sundaralingam, Crystal structure of the complex of bovine pancreatic phospholipase A2 with the inhibitor 1-hexadecyl-3-(trifluoroethyl)-*sn*-glycero-2- phosphomethanol, Biochemistry 36 (1997) 14186–14191.
[20] B.Z. Yu, J. Rogers, G.R. Nicol, K.H. Theopold, K. Seshadri, S. Vishweshwara, M.K. Jain, Catalytic significance of the specificity of

divalent cations as K_S^* and k_{cat}^* cofactors for secreted phospholipase A2, Biochemistry 37 (1998) 12576–12587.
[21] B.J. Bahnson, Structure, function and interfacial allosterism in phospholipase A2: insight from the anion-assisted dimer, Arch. Biochem. Biophys. 43 (2005) 96–106.
[22] Y.H. Pan, T.M. Epstein, M.K. Jain, B.J. Bahnson, Five coplanar anion binding sites on one face of phospholipase A2: relationship to interface binding, Biochemistry 40 (2001) 609–617.
[23] T.M. Epstein, B.Z. Yu, Y.H. Pan, S.P. Tutton, B.P. Maliwal, M.K. Jain, B.J. Bahnson, The basis for k_{cat} impairment in prophospholipase A2 from the anion-assisted dimer structure, Biochemistry 40 (2001) 11411–11422.
[24] M.K. Jain, Introduction to Biological Membranes, 2ndJohn Wiley, New York, 1988.
[25] R.B. Gennis, Biomembranes: Molecular Structure and Function, Springer-Verlag, New York, 1989.
[26] M.K. Jain, G.H. DeHaas, J.F. Marecek, F. Ramirez, The affinity of phospholipase A2 for the interface of the substrate and analogs, Biochim. Biophys. Acta 860 (1986) 475–483.
[27] M.K. Jain, J. Rogers, Substrate specificity for interfacial catalysis by phospholipase A2 in the scooting mode, Biochim. Biophys. Acta 1003 (1989) 91–97.
[28] O.G. Berg, J. Rogers, B.Z. Yu, J. Yao, L.S. Romsted, M.K. Jain, Thermodynamic and kinetic basis of interfacial activation: resolution of binding and allosteric effects on pancreatic phospholipase A2 at zwitterionic interfaces, Biochemistry 36 (1997) 14512–14530.
[29] B.Z. Yu, J. Rogers, M.D. Tsai, C. Pidgeon, M.K. Jain, Contributions of residues of pancreatic phospholipase A2 to interfacial binding, catalysis, and activation, Biochemistry 38 (1999) 4875–4884.
[30] M.J. Janssen, H.M. Verheij, A.J. Slotboom, M.R. Egmond, Engineering the disulphide bond patterns of secretory phospholipases A2 into porcine pancreatic isozyme. The effects on folding, stability and enzymatic properties, Eur. J. Biochem. 261 (1999) 197–207.
[31] M.K. Jain, W.J. Tao, J. Rogers, C. Arenson, H. Eibl, B.Z. Yu, Active-site-directed specific competitive inhibitors of phospholipase A2: novel transition-state analogues, Biochemistry 30 (1991) 10256–10268.
[32] M.K. Jain, J. Rogers, O. Berg, M.H. Gelb, Interfacial catalysis by phospholipase A2: activation by substrate replenishment, Biochemistry 30 (1991) 7340–7348.
[33] M.K. Jain, B.P. Maliwal, Spectroscopic properties of the states of pig pancreatic phospholipase A2 at interfaces and their possible molecular origin [published erratum appears in Biochemistry 1994 Jul 19;33 (28):8618], Biochemistry 32 (1993) 11838–11846.
[34] T.F. Spande, B. Witkop, Determination of the tryptophan content of proteins with N-bromosuccinimide, Methods Enzymol. 11 (1967) 498–506.
[35] B.Z. Yu, O.G. Berg, M.K. Jain, The divalent cation is obligatory for the binding of ligands to the catalytic site of secreted phospholipase A2, Biochemistry 32 (1993) 6485–6492.
[36] X. Liu, H. Zhu, B. Huang, J. Rogers, B.Z. Yu, A. Kumar, M.K. Jain, M. Sundaralingam, M.D. Tsai, Phospholipase A2 engineering. Probing the structural and functional roles of N-terminal residues with site-directed mutagenesis, X-ray, and NMR, Biochemistry 34 (1995) 7322–7334.
[37] B.P. Maliwal, B.Z. Yu, H. Szmacinski, T. Squier, J. van Binsbergen, A.J. Slotboom, M.K. Jain, Functional significance of the conformational dynamics of the N- terminal segment of secreted phospholipase A2 at the interface, Biochemistry 33 (1994) 4509–4516.
[38] H.M. Verheij, M.R. Egmond, G.H. de Haas, Chemical modification of the alpha-amino group in snake venom phospholipases A2. a comparison of the interaction of pancreatic and venom phospholipases with lipid–water interfaces, Biochemistry 20 (1981) 94–99.
[39] O.G. Berg, B.Z. Yu, C. Chang, K.A. Koehler, M.K. Jain, Cooperative binding of monodisperse anionic amphiphiles to the i-face: phospholipase A2-paradigm for interfacial binding, Biochemistry 43 (2004) 7999–8013.
[40] M.K. Jain, G. Ranadive, B.Z. Yu, H.M. Verheij, Interfacial catalysis by phospholipase A2: monomeric enzyme is fully catalytically active at the bilayer interface, Biochemistry 30 (1991) 7330–7340.
[41] S.A. Beers, A.G. Buckland, N. Giles, M.H. Gelb, D.C. Wilton, Effect of tryptophan insertions on the properties of the human group IIA phospholipase A2: mutagenesis produces an enzyme with characteristics similar to those of the human group V phospholipase A2, Biochemistry 42 (2003) 7326–7338.
[42] S.K. Han, K.P. Kim, R. Koduri, L. Bittova, N.M. Munoz, A.R. Leff, D.C. Wilton, M.H. Gelb, W. Cho, Roles of Trp31 in high membrane binding and proinflammatory activity of human group V phospholipase A2, J. Biol. Chem. 274 (1999) 11881–11888.
[43] B.W. Dijkstra, K.H. Kalk, W.G. Hol, J. Drenth, Structure of bovine pancreatic phospholipase A2 at 1.7A resolution, J. Mol. Biol. 147 (1981) 97–123.
[44] D.L. Scott, P.B. Sigler, Structure and catalytic mechanism of secretory phospholipases A2, Adv. Protein Chem. 45 (1994) 53–88.
[45] B.W. Dijkstra, G.J.H. van Nes, K.H. Kalk, N.P. Brandenburg, W.G.J. Hol, J. Drenth, The structure of bovine pancreatic prophospholipase a2 at 3.0 A resolution, Acta Crystallogr. B38 (1982) 793–799.
[46] C. Yuan, M. Tsai, Pancreatic phospholipase A(2): new views on old issues, Biochim. Biophys. Acta 1441 (1999) 215–222.
[47] M.R. Eftink, Fluorescence quenching reactions:probing biological macromolecular structures in Biphysical and Bichemical Aspects of Fluorescence Spectroscopy, in: G. Dewey (Ed.), Plenum Press, New York, 1991, pp. 1–41.
[48] J.R. Lakowicz, Principles of Fluorescence Spectroscopy, Kluwer, New York, 1999.
[49] R. Eksteen, K.J. Pardue, Modified silica-based packing materials for size exclusion chromatography, in: C. Wu (Ed.), Handbook of Size Exclusion Chromatography and Related Techniques, Marcel Dekker, Inc., New York, 2004, pp. 45–98.
[50] Y.H. Pan, B.Z. Yu, O.G. Berg, M.K. Jain, B.J. Bahnson, Crystal structure of phospholipase A2 complex with the hydrolysis products of platelet activating factor: equilibrium binding of fatty acid and lysophospholipid-ether at the active site may be mutually exclusive, Biochemistry 41 (2002) 14790–14800.
[51] L.S. Romsted, Micellar Effects on Reaction Rates and Equilibria, vol. 2, Plenum Press, New York, 1984.
[52] Y. Geng, L.S. Romsted, D. Zanette, L. Magid, I.M. Cuccovia, H. Chaimovich, Origin of the sphere-to-rod transition in cationic micelles with aromatic counterions: Specific ion hydration in the interfacial region matter, Labgmuir 21 (2005) 562–568.
[53] R. Ramachandrappa, S. Putta, S.M. Mayanna, N.M.M. Gowda, Kinetics and mechanism of oxidation of aspirin by bromamine-TN-bromosuccinimide, an N-bromophthalimide, Int. J. Chem. Kinet. 30 (1998).
[54] R. Verger, G.H. de Haas, Interfacial enzyme kinetics of lipolysis, Ann. Rev. Biophys. Bioeng. 5 (1976) 77–117.
[55] Y. Cajal, O.G. Berg, M.K. Jain, Direct vesicle–vesicle exchange of phospholipids mediated by polymyxin B, Biochem. Biophys. Res. Commun. 210 (1995) 746–752.
[56] M.K. Jain, J. Rogers, J.F. Marecek, F. Ramirez, H. Eibl, Effect of the structure of phospholipid on the kinetics of intravesicle scooting of phospholipase A2, Biochim. Biophys. Acta 860 (1986) 462–474.
[57] Y. Cajal, M.K. Jain, Synergism between mellitin and phospholipase A2 from bee venom: apparent activation by intervesicle exchange of phospholipids, Biochemistry 36 (1997) 3882–3893.
[58] B.Z. Yu, R. Apitz-Castro, M.D. Tsai, M.K. Jain, Interaction of monodisperse anionic amphiphiles with the i-face of secreted phospholipase A2, Biochemistry 42 (2003) 6293–6301.
[59] F. Zhou, K. Schulten, Molecular dynamics study of phospholipase A2 on a membrane surface, Proteins 25 (1996) 12–27.
[60] S. Quin, A.H. Pande, K.N. Nemec, S.A. Tatulian, The N-terminal a-helix of pancreatic phospholipase A2 determines productive-mode orientation of the enzyme at the membrane surface, J. Mol. Biol. 344 (2004) 71–89.
[61] P.D. Adams, Y. Chen, K. Ma, M.G. Zagorski, F.D. Sonnichsen, M.L. McLaughlin, M.D. Barkley, intramolecular quenching of tryptophan fluorescence by the peptide bond in cyclic hexapeptides, J. Am. Chem. Soc. 124 (2002) 9278–9286.
[62] M.C. Moncrieffe, N. Juranic, M.D. Kemple, J.D. Potter, S. Macura, F.G. Pendergast, Structure–fluorescence correlations in a single tryptophan

mutant of carp paralbumin: solution structure, backbone and side-chain dynamics, J. Mol. Biol. 297 (2000) 147–163.
[63] A.G. Szabo, D.M. Rayner, Fluorescence decay of tryptophan conformers in aqueous solution, J. Am. Chem. Soc. 102 (1980) 554–563.
[64] J.M. Beechem, L. Brand, Time-resolved fluorescence of proteins, Annu. Rev. Biochem. 54 (1985) 43–71.
[65] B.Z. Yu, F. Ghomashchi, Y. Cajal, R.R. Annand, O.G. Berg, M.H. Gelb, M.K. Jain, Use of an imperfect neutral diluent and outer vesicle layer scooting mode hydrolysis to analyze the interfacial kinetics, inhibition, and substrate preferences of bee venom phospholipase A2, Biochemistry 36 (1997) 3870–3881.
[66] M.K. Jain, M.R. Egmond, H.M. Verheij, R. Apitz-Castro, R. Dijkman, G.H. De Haas, Interaction of phospholipase A2 and phospholipid bilayers, Biochim. Biophys. Acta 688 (1982) 341–348.